

Measurement of the Differential Cross Section for Events with Large Total Transverse Energy in $p\bar{p}$ Collisions at $\sqrt{s} = 1.8$ TeV

F. Abe,¹⁷ H. Akimoto,³⁹ A. Akopian,³¹ M. G. Albrow,⁷ A. Amadon,⁵ S. R. Amendolia,²⁷ D. Amidei,²⁰ J. Antos,³³ S. Aota,³⁷ G. Apollinari,³¹ T. Arisawa,³⁹ T. Asakawa,³⁷ W. Ashmanskas,¹⁸ M. Atac,⁷ P. Azzi-Bacchetta,²⁵ N. Bacchetta,²⁵ S. Bagdasarov,³¹ M. W. Bailey,²² P. de Barbaro,³⁰ A. Barbaro-Galtieri,¹⁸ V. E. Barnes,²⁹ B. A. Barnett,¹⁵ M. Barone,⁹ G. Bauer,¹⁹ T. Baumann,¹¹ F. Bedeschi,²⁷ S. Behrends,³ S. Belforte,²⁷ G. Bellettini,²⁷ J. Bellinger,⁴⁰ D. Benjamin,³⁵ J. Bensinger,³ A. Beretvas,⁷ J. P. Berge,⁷ J. Berryhill,⁵ S. Bertolucci,⁹ S. Bettelli,²⁷ B. Bevensee,²⁶ A. Bhatti,³¹ K. Biery,⁷ C. Bigongiari,²⁷ M. Binkley,⁷ D. Bisello,²⁵ R. E. Blair,¹ C. Blocker,³ S. Blusk,³⁰ A. Bodek,³⁰ W. Bokhari,²⁶ G. Bolla,²⁹ Y. Bonushkin,⁴ D. Bortoletto,²⁹ J. Boudreau,²⁸ L. Breccia,² C. Bromberg,²¹ N. Bruner,²² R. Brunetti,² E. Buckley-Geer,⁷ H. S. Budd,³⁰ K. Burkett,²⁰ G. Busetto,²⁵ A. Byon-Wagner,⁷ K. L. Byrum,¹ M. Campbell,²⁰ A. Caner,²⁷ W. Carithers,¹⁸ D. Carlsmith,⁴⁰ J. Cassada,³⁰ A. Castro,²⁵ D. Cauz,³⁶ A. Cerri,²⁷ P. S. Chang,³³ P. T. Chang,³³ H. Y. Chao,³³ J. Chapman,²⁰ M.-T. Cheng,³³ M. Chertok,³⁴ G. Chiarelli,²⁷ C. N. Chiou,³³ F. Chlebana,⁷ L. Christofek,¹³ M. L. Chu,³³ S. Cihangir,⁷ A. G. Clark,¹⁰ M. Cobal,²⁷ E. Cocca,²⁷ M. Contreras,⁵ J. Conway,³² J. Cooper,⁷ M. Cordelli,⁹ D. Costanzo,²⁷ C. Couyoumtzelis,¹⁰ D. Cronin-Hennessy,⁶ R. Culbertson,⁵ D. Dagenhart,³⁸ T. Daniels,¹⁹ F. DeJongh,⁷ S. Dell'Agnello,⁹ M. Dell'Orso,²⁷ R. Demina,⁷ L. Demortier,³¹ M. Deninno,² P. F. Derwent,⁷ T. Devlin,³² J. R. Dittmann,⁶ S. Donati,²⁷ J. Done,³⁴ T. Dorigo,²⁵ N. Eddy,²⁰ K. Einsweiler,¹⁸ J. E. Elias,⁷ R. Ely,¹⁸ E. Engels, Jr.,²⁸ W. Erdmann,⁷ D. Errede,¹³ S. Errede,¹³ Q. Fan,³⁰ R. G. Feild,⁴¹ Z. Feng,¹⁵ C. Ferretti,²⁷ I. Fiori,² B. Flaughner,⁷ G. W. Foster,⁷ M. Franklin,¹¹ J. Freeman,⁷ J. Friedman,¹⁹ H. Frisch,⁵ Y. Fukui,¹⁷ S. Gadomski,¹⁴ S. Galeotti,²⁷ M. Gallinaro,²⁶ O. Ganel,³⁵ M. Garcia-Sciveres,¹⁸ A. F. Garfinkel,²⁹ C. Gay,⁴¹ S. Geer,⁷ D. W. Gerdes,¹⁵ P. Giannetti,²⁷ N. Giokaris,³¹ P. Giromini,⁹ G. Giusti,²⁷ M. Gold,²² A. Gordon,¹¹ A. T. Goshaw,⁶ Y. Gotra,²⁵ K. Goulianos,³¹ H. Grassmann,³⁶ L. Groer,³² C. Grosso-Pilcher,⁵ G. Guillian,²⁰ J. Guimaraes da Costa,¹⁵ R. S. Guo,³³ C. Haber,¹⁸ E. Hafen,¹⁹ S. R. Hahn,⁷ R. Hamilton,¹¹ T. Handa,¹² R. Handler,⁴⁰ F. Happacher,⁹ K. Hara,³⁷ A. D. Hardman,²⁹ R. M. Harris,⁷ F. Hartmann,¹⁶ J. Hauser,⁴ E. Hayashi,³⁷ J. Heinrich,²⁶ W. Hao,³⁵ B. Hinrichsen,¹⁴ K. D. Hoffman,²⁹ M. Hohlmann,⁵ C. Holck,²⁶ R. Hollebeek,²⁶ L. Holloway,¹³ Z. Huang,²⁰ B. T. Huffman,²⁸ R. Hughes,²³ J. Huston,²¹ J. Huth,¹¹ H. Ikeda,³⁷ M. Incagli,²⁷ J. Incandela,⁷ G. Introzzi,²⁷ J. Iwai,³⁹ Y. Iwata,¹² E. James,²⁰ H. Jensen,⁷ U. Joshi,⁷ E. Kajfasz,²⁵ H. Kambara,¹⁰ T. Kamon,³⁴ T. Kaneko,³⁷ K. Karr,³⁸ H. Kasha,⁴¹ Y. Kato,²⁴ T. A. Keaffaber,²⁹ K. Kelley,¹⁹ R. D. Kennedy,⁷ R. Kephart,⁷ D. Kestenbaum,¹¹ D. Khazins,⁶ T. Kikuchi,³⁷ B. J. Kim,²⁷ H. S. Kim,¹⁴ S. H. Kim,³⁷ Y. K. Kim,¹⁸ L. Kirsch,³ S. Klimenko,⁸ D. Knoblauch,¹⁶ P. Koehn,²³ A. Königeter,¹⁶ K. Kondo,³⁷ J. Konigsberg,⁸ K. Kordas,¹⁴ A. Korytov,⁸ E. Kovacs,¹ W. Kowald,⁶ J. Kroll,²⁶ M. Kruse,³⁰ S. E. Kuhlmann,¹ E. Kuns,³² K. Kurino,¹² T. Kuwabara,³⁷ A. T. Laasanen,²⁹ I. Nakano,¹² S. Lami,²⁷ S. Lammel,⁷ J. I. Lamoureux,³ M. Lancaster,¹⁸ M. Lanzoni,²⁷ G. Latino,²⁷ T. LeCompte,¹ S. Leone,²⁷ J. D. Lewis,⁷ P. Limon,⁷ M. Lindgren,⁴ T. M. Liss,¹³ J. B. Liu,³⁰ Y. C. Liu,³³ N. Lockyer,²⁶ O. Long,²⁶ C. Loomis,³² M. Loretì,²⁵ D. Lucchesi,²⁷ P. Lukens,⁷ S. Lusin,⁴⁰ J. Lys,¹⁸ K. Maeshima,⁷ P. Maksimovic,¹⁹ M. Mangano,²⁷ M. Mariotti,²⁵ J. P. Marriner,⁷ A. Martin,⁴¹ J. A. J. Matthews,²² P. Mazzanti,² P. McIntyre,³⁴ P. Melese,³¹ M. Menguzzato,²⁵ A. Menzione,²⁷ E. Meschi,²⁷ S. Metzler,²⁶ C. Miao,²⁰ T. Miao,⁷ G. Michail,¹¹ R. Miller,²¹ H. Minato,³⁷ S. Miscetti,⁹ M. Mishina,¹⁷ S. Miyashita,³⁷ N. Moggi,²⁷ E. Moore,²² Y. Morita,¹⁷ A. Mukherjee,⁷ T. Muller,¹⁶ P. Murat,²⁷ S. Murgia,²¹ H. Nakada,³⁷ I. Nakano,¹² C. Nelson,⁷ D. Neuberger,¹⁶ C. Newman-Holmes,⁷ C.-Y. P. Ngan,¹⁹ L. Nodulman,¹ S. H. Oh,⁶ T. Ohmoto,¹² T. Ohsugi,¹² R. Oishi,³⁷ M. Okabe,³⁷ T. Okusawa,²⁴ J. Olsen,⁴⁰ C. Pagliarone,²⁷ R. Paoletti,²⁷ V. Papadimitriou,³⁵ S. P. Pappas,⁴¹ N. Parashar,²⁷ A. Parri,⁹ J. Patrick,⁷ G. Pauletta,³⁶ M. Paulini,¹⁸ A. Perazzo,²⁷ L. Pescara,²⁵ M. D. Peters,¹⁸ T. J. Phillips,⁶ G. Piacentino,²⁷ M. Pillai,³⁰ K. T. Pitts,⁷ R. Plunkett,⁷ L. Pondrom,⁴⁰ J. Proudfoot,¹ F. Ptohos,¹¹ G. Punzi,²⁷ K. Ragan,¹⁴ D. Reher,¹⁸ M. Reischl,¹⁶ A. Ribon,²⁵ F. Rimondi,² L. Ristori,²⁷ W. J. Robertson,⁶ T. Rodrigo,²⁷ S. Rolli,³⁸ L. Rosenson,¹⁹ R. Roser,¹³ T. Saab,¹⁴ W. K. Sakumoto,³⁰ D. Saltzberg,⁴ A. Sansoni,⁹ L. Santi,³⁶ H. Sato,³⁷ P. Schlabach,⁷ E. E. Schmidt,⁷ M. P. Schmidt,⁴¹ A. Scott,⁴ A. Scribano,²⁷ S. Segler,⁷ S. Seidel,²² Y. Seiya,³⁷ F. Semeria,² T. Shah,¹⁹ M. D. Shapiro,¹⁸ N. M. Shaw,²⁹ P. F. Shepard,²⁸ T. Shibayama,³⁷ M. Shimojima,³⁷ M. Shochet,⁵ J. Siegrist,¹⁸ A. Sill,³⁵ P. Sinervo,¹⁴ P. Singh,¹³ K. Sliwa,³⁸ C. Smith,¹⁵ F. D. Snider,¹⁵ J. Spalding,⁷ T. Speer,¹⁰ P. Sphicas,¹⁹ F. Spinella,²⁷ M. Spiropulu,¹¹ L. Spiegel,⁷ L. Stanco,²⁵ J. Steele,⁴⁰ A. Stefanini,²⁷ R. Ströhmer,^{7,*} J. Strologas,¹³ F. Strumia,¹⁰ D. Stuart,⁷ K. Sumorok,¹⁹ J. Suzuki,³⁷ T. Suzuki,³⁷ T. Takahashi,²⁴ T. Takano,²⁴ R. Takashima,¹² K. Takikawa,³⁷ M. Tanaka,³⁷ B. Tannenbaum,²² F. Tartarelli,²⁷ W. Taylor,¹⁴ M. Tecchio,²⁰ P. K. Teng,³³ Y. Teramoto,²⁴ K. Terashi,³⁷ S. Tether,¹⁹ D. Theriot,⁷ T. L. Thomas,²² R. Thurman-Keup,¹

M. Timko,³⁸ P. Tipton,³⁰ A. Titov,³¹ S. Tkaczyk,⁷ D. Toback,⁵ K. Tollefson,¹⁹ A. Tollestrup,⁷ H. Toyoda,²⁴
 W. Trischuk,¹⁴ J. F. de Troconiz,¹¹ S. Truitt,²⁰ J. Tseng,¹⁹ N. Turini,²⁷ T. Uchida,³⁷ F. Ukegawa,²⁶ J. Valls,³²
 S. C. van den Brink,²⁸ S. Vejcik III,²⁰ G. Velev,²⁷ R. Vidal,⁷ R. Vilar,^{7,*} D. Vucinic,¹⁹ R. G. Wagner,¹ R. L. Wagner,⁷
 J. Wahl,⁵ N. B. Wallace,²⁷ A. M. Walsh,³² C. Wang,⁶ C. H. Wang,³³ M. J. Wang,³³ A. Warburton,¹⁴ T. Watanabe,³⁷
 T. Watts,³² R. Webb,³⁴ C. Wei,⁶ H. Wenzel,¹⁶ W. C. Wester III,⁷ A. B. Wicklund,¹ E. Wicklund,⁷ R. Wilkinson,²⁶
 H. H. Williams,²⁶ P. Wilson,⁵ B. L. Winer,²³ D. Winn,²⁰ D. Wolinski,²⁰ J. Wolinski,²¹ S. Worm,²² X. Wu,¹⁰ J. Wyss,²⁷
 A. Yagil,⁷ W. Yao,¹⁸ K. Yasuoka,³⁷ G. P. Yeh,⁷ P. Yeh,³³ J. Yoh,⁷ C. Yosef,²¹ T. Yoshida,²⁴ I. Yu,⁷ A. Zanetti,³⁶
 F. Zetti,²⁷ and S. Zucchelli²

(CDF Collaboration)

¹Argonne National Laboratory, Argonne, Illinois 60439

²Istituto Nazionale di Fisica Nucleare, University of Bologna, I-40127 Bologna, Italy

³Brandeis University, Waltham, Massachusetts 02254

⁴University of California at Los Angeles, Los Angeles, California 90024

⁵University of Chicago, Chicago, Illinois 60637

⁶Duke University, Durham, North Carolina 27708

⁷Fermi National Accelerator Laboratory, Batavia, Illinois 60510

⁸University of Florida, Gainesville, Florida 32611

⁹Laboratori Nazionali di Frascati, Istituto Nazionale di Fisica Nucleare, I-00044 Frascati, Italy

¹⁰University of Geneva, CH-1211 Geneva 4, Switzerland

¹¹Harvard University, Cambridge, Massachusetts 02138

¹²Hiroshima University, Higashi-Hiroshima 724, Japan

¹³University of Illinois, Urbana, Illinois 61801

¹⁴Institute of Particle Physics, McGill University, Montreal H3A 2T8

and University of Toronto, Toronto M5S 1A7, Canada

¹⁵The Johns Hopkins University, Baltimore, Maryland 21218

¹⁶Institut für Experimentelle Kernphysik, Universität Karlsruhe, 76128 Karlsruhe, Germany

¹⁷National Laboratory for High Energy Physics (KEK), Tsukuba, Ibaraki 305, Japan

¹⁸Ernest Orlando Lawrence Berkeley National Laboratory, Berkeley, California 94720

¹⁹Massachusetts Institute of Technology, Cambridge, Massachusetts 02139

²⁰University of Michigan, Ann Arbor, Michigan 48109

²¹Michigan State University, East Lansing, Michigan 48824

²²University of New Mexico, Albuquerque, New Mexico 87131

²³The Ohio State University, Columbus, Ohio 43210

²⁴Osaka City University, Osaka 588, Japan

²⁵Università di Padova, Istituto Nazionale di Fisica Nucleare, Sezione di Padova, I-35131 Padova, Italy

²⁶University of Pennsylvania, Philadelphia, Pennsylvania 19104

²⁷Istituto Nazionale di Fisica Nucleare, University and Scuola Normale Superiore of Pisa, I-56100 Pisa, Italy

²⁸University of Pittsburgh, Pittsburgh, Pennsylvania 15260

²⁹Purdue University, West Lafayette, Indiana 47907

³⁰University of Rochester, Rochester, New York 14627

³¹Rockefeller University, New York, New York 10021

³²Rutgers University, Piscataway, New Jersey 08855

³³Academia Sinica, Taipei, Taiwan 11530, Republic of China

³⁴Texas A&M University, College Station, Texas 77843

³⁵Texas Tech University, Lubbock, Texas 79409

³⁶Istituto Nazionale di Fisica Nucleare, University of Trieste/Udine, Italy

³⁷University of Tsukuba, Tsukuba, Ibaraki 315, Japan

³⁸Tufts University, Medford, Massachusetts 02155

³⁹Waseda University, Tokyo 169, Japan

⁴⁰University of Wisconsin, Madison, Wisconsin 53706

⁴¹Yale University, New Haven, Connecticut 06520

(Received 18 August 1997)

We present a measurement of the differential cross section $d\sigma/d\sum E_T^{\text{jet}}$ for the production of multijet events in $p\bar{p}$ collisions where the sum is over all jets with transverse energy $E_T^{\text{jet}} > E_T^{\text{min}}$. The measured cross section for events with $\sum E_T^{\text{jet}} > 320$ GeV is compared to $\mathcal{O}(\alpha_s^3)$ perturbative QCD predictions and QCD parton shower Monte Carlo predictions. The agreement between the $\mathcal{O}(\alpha_s^3)$ predicted and observed event rates is reasonable for $E_T^{\text{min}} = 100$ GeV, but poorer for $E_T^{\text{min}} = 20$ GeV. [S0031-9007(98)05889-X]

PACS numbers: 13.87.Ce, 12.38.Qk

Within the framework of perturbative QCD, events with large total transverse energy are expected to be produced in $p\bar{p}$ collisions from hard parton-parton scattering. The outgoing scattered partons manifest themselves as hadronic jets. The lowest order QCD diagrams predict two jets in the final state. Higher order processes can give rise to events with more than two jets. The kinematic properties of events with up to six jets [1–3] and large total transverse energy have been previously measured by the CDF Collaboration at the Tevatron $p\bar{p}$ collider operating at a center-of-mass energy of 1.8 TeV. The kinematic properties of these multijet events are well described by both the HERWIG [4] QCD parton shower Monte Carlo program and the NJETS [5] complete leading order (LO) QCD matrix element Monte Carlo program for $2 \rightarrow N$ scattering. In the present Letter we extend our results by comparing the differential cross section for multijet events with large total transverse energy to predictions from the HERWIG Monte Carlo program and the JETRAD next to leading order (NLO) two-jet Monte Carlo program [6].

The data used in the present analysis were recorded by the CDF experiment over the period 1992–1995 and correspond to an integrated luminosity of $112 \pm 8 \text{ pb}^{-1}$ [7]. A full description of the CDF detector can be found in Ref. [8]. The analysis described in this Letter exploits the CDF calorimeters which cover the pseudorapidity region $|\eta| < 4.2$, where $\eta \equiv -\ln(\tan \theta/2)$. The calorimeters are constructed in a tower geometry in η - ϕ space (ϕ is the azimuthal angle around the beam line). The towers are 0.1 units wide in η and 15° wide in ϕ in the central region and 5° wide at larger η (approximately $|\eta| > 1.2$).

The data were recorded using a trigger that required $\sum E_T^{\text{cluster}} > 175 \text{ GeV}$, where the sum is over all calorimeter clusters found by the hardware trigger processor which reconstructed clusters with an effective minimum E_T^{cluster} of 3 GeV. To reject backgrounds from cosmic ray interactions, beam halo, and detector malfunctions, the events were required to have: (i) total energy less than 2000 GeV, (ii) no significant energy deposited in the hadron calorimeters out-of-time with the proton-antiproton collision, (iii) missing E_T (\cancel{E}_T) significance [1] $S \equiv \cancel{E}_T / (\sum E_T^{\text{towers}})^{1/2} < 6 \text{ GeV}^{1/2}$, where the sum is over all calorimeter towers above a given threshold, and (iv) a primary vertex reconstructed with $|z| < 60 \text{ cm}$. The measured cross section is corrected for the efficiency

TABLE I. Parameters for the fit to the unsmeared $\sum E_T^{\text{jet}}$ spectra using Eq. (1).

Parameter	$E_T^{\text{min}} = 20 \text{ GeV}$	$E_T^{\text{min}} = 100 \text{ GeV}$
p_1	-4.905	-7.490
p_2	0.868	0.864
p_3	-0.099	-0.130
p_4	-0.097	-0.053
p_5	0.013	0.023
p_6	5.586	11.998
$A \text{ (pb/GeV)}$	8.030×10^{12}	1.874×10^{17}

of the primary vertex cut. The cut on total energy rejects 0.8% of genuine $p\bar{p}$ interactions while the remaining cuts are essentially 100% efficient. These requirements select 749 506 events for further analysis.

Jets are reconstructed using a cone algorithm [9] with radius $R \equiv (\Delta\eta^2 + \Delta\phi^2)^{1/2} = 0.7$. Jet energies are corrected [9] for calorimeter nonlinearities, energy lost in uninstrumented regions, and energy that falls inside the clustering cone from the fragmentation of partons not associated with the hard scatter. The typical correction is 18% for jets of $E_T^{\text{jet}} = 200 \text{ GeV}$ falling to 13% for jets of $E_T^{\text{jet}} = 400 \text{ GeV}$. We do not correct for energy that falls outside the clustering

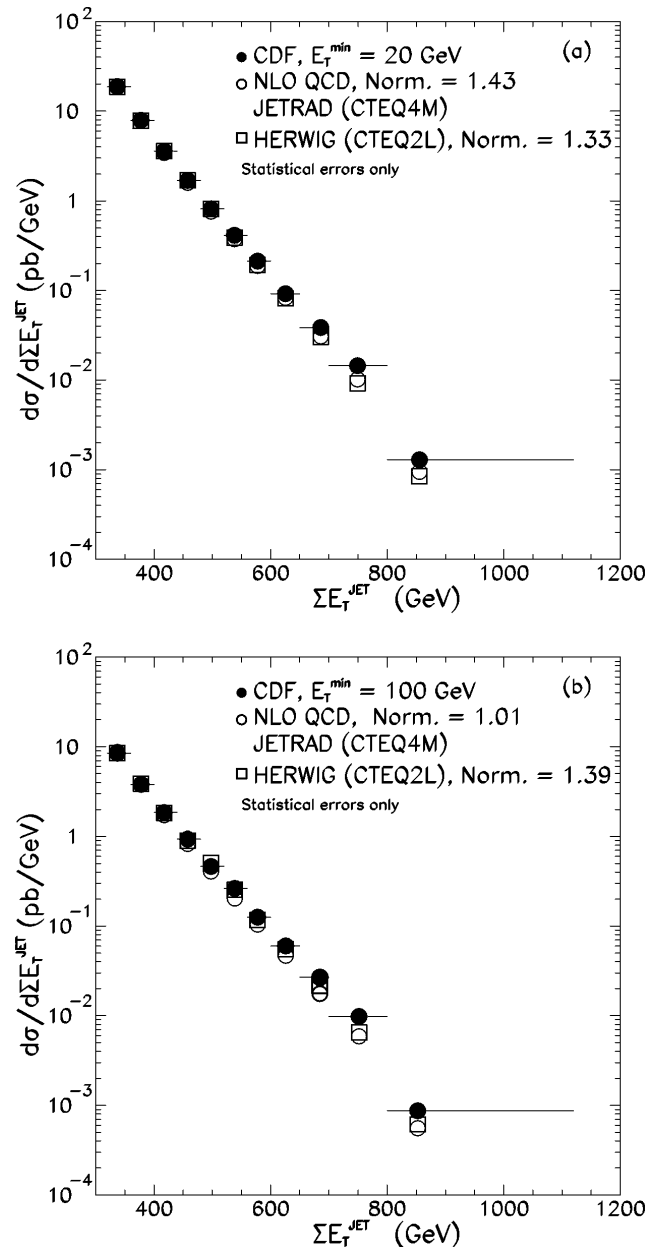


FIG. 1. The unsmeared $\sum E_T^{\text{jet}}$ differential cross section compared to the predictions from HERWIG and from NLO QCD for (a) $E_T^{\text{min}} = 20 \text{ GeV}$ and (b) $E_T^{\text{min}} = 100 \text{ GeV}$.

cone because this is taken into account by the parton shower in the HERWIG Monte Carlo program and also to some degree in the NLO QCD calculations.

We measure the differential cross section for events with large total transverse energy, $d\sigma/d\sum E_T^{\text{jet}}$, where the sum is over all jets above a given E_T^{min} after jet energy corrections have been applied. The cross section has been measured for two different choices of E_T^{min} , $E_T^{\text{min}} = 20$ GeV [$E_T^{\text{min}}(20)$], and $E_T^{\text{min}} = 100$ GeV [$E_T^{\text{min}}(100)$]. When we refer to both samples together the number in parentheses refers to the $E_T^{\text{min}}(100)$ sample. Events with $\sum E_T^{\text{jet}} > 320$ GeV are retained (the trigger is fully efficient for events above this $\sum E_T^{\text{jet}}$ threshold for both choices of E_T^{min}), yielding a sample of 141 041(71 611) events.

The measured $\sum E_T^{\text{jet}}$ spectrum must be corrected for smearing effects caused by the finite experimental E_T^{jet} resolution. To determine the $\sum E_T^{\text{jet}}$ resolution of the detector we have used a sample of HERWIG Monte Carlo events that have been passed through the CDF detector simulation. The $\sum E_T^{\text{jet}}$ resolution varies between 8% and 10% over the $\sum E_T^{\text{jet}}$ range of interest for both choices of E_T^{min} .

The predicted $\sum E_T^{\text{jet}}$ spectra can be parametrized using the following functional form:

$$\frac{d\sigma}{d\sum E_T^{\text{jet}}} = A \times \left(1 - \sum E_T^{\text{jet}}/\sqrt{s}\right)^{p_6} \times 10^f, \quad (1)$$

where $f = \sum_{i=1}^5 p_i \log_{10}(\sum E_T^{\text{jet}})$. We convolute this parametrization with the resolution function and compare it to the observed spectra. The best fits to the observed spectra obtained with the parameters listed in Table I which yield a χ^2 of 30(36) for 28 degrees of freedom. To unsmear the observed spectrum, we compare the fitted functional forms before and after they are convoluted with the resolution function. This yields a bin-by-bin unsmearing correction that is applied to the cross section in each bin of measured $\sum E_T^{\text{jet}}$. Typical unsmearing corrections for $\sum E_T^{\text{jet}} = 320$ GeV

are 1.025(0.97) and for $\sum E_T^{\text{jet}} = 900$ GeV are 0.94(0.87). The unsmearing cross sections along with the statistical uncertainties are shown in Fig. 1 and given in Table II.

The systematic uncertainties on the cross section arise from the following sources:

(a) The uncertainty on the absolute energy scale of the calorimeters. The one standard deviation systematic uncertainty on the energy scale is 5.6% at $E_T^{\text{jet}} = 20$ GeV dropping to 3.4% at $E_T^{\text{jet}} = 100$ GeV [10]. For jets in the rapidity range $1.4 < |\eta| < 2.4$ there is an additional 2% uncertainty on the energy scale relative to the central calorimeter. To evaluate the uncertainty on the measured differential cross section due to this uncertainty we changed the jet energies by one systematic standard deviation and recalculated the unsmearing correction. Note that a small change in the jet energy can cause jets to be eliminated from or included in the $\sum E_T^{\text{jet}}$ for the event. This effect is included in our evaluation of the systematic uncertainty and results in a much larger uncertainty on $d\sigma/d\sum E_T^{\text{jet}}$ than, for example, the corresponding uncertainty on the inclusive jet cross section $d\sigma/dE_T^{\text{jet}}$ [11].

(b) The modeling of the resolution functions. The resolution functions have a non-Gaussian tail due to calorimeter nonlinearities and energy lost in uninstrumented regions. To estimate the uncertainty on the measured cross section due to our imperfect knowledge of the tails we have recalculated the unsmearing corrections using resolution functions in which the non-Gaussian tails have been (i) eliminated and (ii) doubled.

(c) An overall normalization uncertainty of 7% derived from the uncertainty in the luminosity measurement.

The fractional changes in the cross section due to changes in absolute energy scale and/or resolutions functions are given by $\Delta\sigma(\sum E_T^{\text{jet}})/\sigma(\sum E_T^{\text{jet}}) = a \sum E_T^{\text{jet}} + b$. The values of a and b corresponding to one standard deviation changes are shown in Table III. The overall systematic uncertainty is obtained by combining the individual contributions due to absolute energy scale,

TABLE II. $d\sigma/d\sum E_T^{\text{jet}}$. The $\langle\sum E_T^{\text{jet}}\rangle$ is the mean value within a bin and the uncertainties are statistical only.

Bin (GeV)	$\langle\sum E_T^{\text{jet}}\rangle$ (GeV)	$E_T^{\text{min}} = 20$ GeV		$E_T^{\text{min}} = 100$ GeV	
		$d\sigma/d\sum E_T^{\text{jet}}$ (pb/GeV)	$\langle\sum E_T^{\text{jet}}\rangle$ (GeV)	$d\sigma/d\sum E_T^{\text{jet}}$ (pb/GeV)	$\langle\sum E_T^{\text{jet}}\rangle$ (GeV)
320–360	337.2	$(1.86 \pm 0.01) \times 10^1$	337.2	$(8.49 \pm 0.04) \times 10^0$	
360–400	377.4	$(7.90 \pm 0.04) \times 10^0$	377.6	$(3.80 \pm 0.03) \times 10^0$	
400–440	417.6	$(3.59 \pm 0.03) \times 10^0$	417.6	$(1.84 \pm 0.02) \times 10^0$	
440–480	457.5	$(1.69 \pm 0.02) \times 10^0$	457.7	$(9.34 \pm 0.15) \times 10^{-1}$	
480–520	497.7	$(8.10 \pm 0.14) \times 10^{-1}$	497.8	$(4.63 \pm 0.10) \times 10^{-1}$	
520–560	538.0	$(4.11 \pm 0.10) \times 10^{-1}$	538.3	$(2.63 \pm 0.08) \times 10^{-1}$	
560–600	577.6	$(2.13 \pm 0.07) \times 10^{-1}$	577.7	$(1.25 \pm 0.05) \times 10^{-1}$	
600–650	625.6	$(9.21 \pm 0.38) \times 10^{-2}$	625.8	$(6.02 \pm 0.3) \times 10^{-2}$	
650–700	686.1	$(3.84 \pm 0.24) \times 10^{-2}$	684.6	$(2.68 \pm 0.2) \times 10^{-2}$	
700–800	749.3	$(1.43 \pm 0.13) \times 10^{-2}$	751.5	$(9.77 \pm 1.03) \times 10^{-3}$	
800–1120	855.3	$(1.29 \pm 0.18) \times 10^{-3}$	852.3	$(8.74 \pm 1.44) \times 10^{-4}$	

resolution functions, and luminosity uncertainties in quadrature (also shown in Table III).

The measured total cross section for $\sum E_T^{\text{jet}} > 320$ GeV is $1.34^{+0.44}_{-0.36}$ nb for $E_T^{\text{min}}(20)$ and $0.64^{+0.17}_{-0.15}$ nb for $E_T^{\text{min}}(100)$. The quoted uncertainties are the one standard deviation systematic uncertainties (the statistical uncertainties are negligible). The differential cross sections are compared to NLO QCD predictions in Fig. 1. This is a next-to-leading order $2 \rightarrow 2$ calculation using the CTEQ4M parton distribution functions (PDFs) [12] and a renormalization and factorization scale of $\mu = 0.5 \sum E_T^{\text{jet}}$. We also compare the data to predictions from the HERWIG parton shower Monte Carlo program [4]. The HERWIG curve was generated using CTEQ2L parton distributions and a scale of $Q^2 = stu/2(s^2 + t^2 + u^2)$ for the hard $2 \rightarrow 2$ process. In Fig. 1 the QCD predictions have been normalized to the data between $\sum E_T^{\text{jet}} = 320 - 480$ GeV for both choices of E_T^{min} . For $E_T^{\text{min}}(20)$, this yields a normalization $F = 1.43$ for the NLO QCD prediction using the CTEQ4M PDF (corresponding to 1.14 standard deviations). The large normalization factor suggests that the NLO $2 \rightarrow 2$ calculation is not adequate to describe the rate of events at large $\sum E_T^{\text{jet}}$. We note that for $E_T^{\text{min}}(20)$ there are more three-jet events than two-jet events in our $\sum E_T^{\text{jet}} > 320$ GeV data sample [2], which suggests that $\mathcal{O}(\alpha_s^4)$ corrections to the NLO $2 \rightarrow 2$ calculation may be important. In this sample 31% of the events have more than three jets passing the E_T^{min} cut. For $E_T^{\text{min}}(100)$ the normalization $F = 1.01$ for the NLO QCD prediction suggests that the NLO calculation can better describe the data once we are in a region where two-jet events dominate. In this sample 95% of the events have only two jets passing the E_T^{min} cut (this fraction falls to about 78% for $\sum E_T^{\text{jet}} > 600$ GeV).

We have studied the effect on the predicted cross section of varying μ . Using $\mu = 0.25 \sum E_T^{\text{jet}}$ we obtain a normalization $F = 1.15$ for $E_T^{\text{min}}(20)$ and $F = 0.95$ for $E_T^{\text{min}}(100)$. The large change in normalization for $E_T^{\text{min}}(20)$ suggests that the higher order corrections are significant, while the change seen for $E_T^{\text{min}}(100)$ is typical of NLO calculations. The normalization factor for the HERWIG prediction is large for both choices of E_T^{min} , namely $F = 1.33(1.39)$. This is to be expected because

TABLE III. Summary of the coefficients a and b for $\Delta\sigma(\sum E_T^{\text{jet}})/\sigma(\sum E_T^{\text{jet}}) = a \sum E_T^{\text{jet}} + b$. The fractional systematic uncertainties listed are the energy scale, resolution function, and the total.

Systematic uncertainty	$E_T^{\text{min}} = 20$ GeV		$E_T^{\text{min}} = 100$ GeV	
	a (GeV ⁻¹)	b	a (GeV ⁻¹)	b
Energy scale (+)	1.44×10^{-4}	0.251	1.62×10^{-4}	0.193
Energy scale (-)	1.12×10^{-4}	0.200	3.11×10^{-4}	0.090
Resolution (+/-)	1.16×10^{-4}	0.045	2.08×10^{-4}	-0.019
Total (+)	1.72×10^{-4}	0.261	2.22×10^{-4}	0.188
Total (-)	1.46×10^{-4}	0.213	3.56×10^{-4}	0.094

although HERWIG includes a parton shower, the underlying hard scattering cross section is only LO $2 \rightarrow 2$.

The observed spectra are harder than the NLO QCD and HERWIG predictions above about 500 GeV for both choices of E_T^{min} . This effects is similar to the one observed in the inclusive jet differential cross section [11] for $E_T^{\text{jet}} > 200$ GeV as reported by the CDF Collaboration. It can be seen more clearly in Fig. 2 where we show the ratio of the data divided by the theoretical predictions. The theory has not been normalized to the data allowing both the normalization and the shape to be compared. The systematic uncertainty is shown relative to the solid circles (NLO QCD and CTEQ4M parton distributions). Comparisons

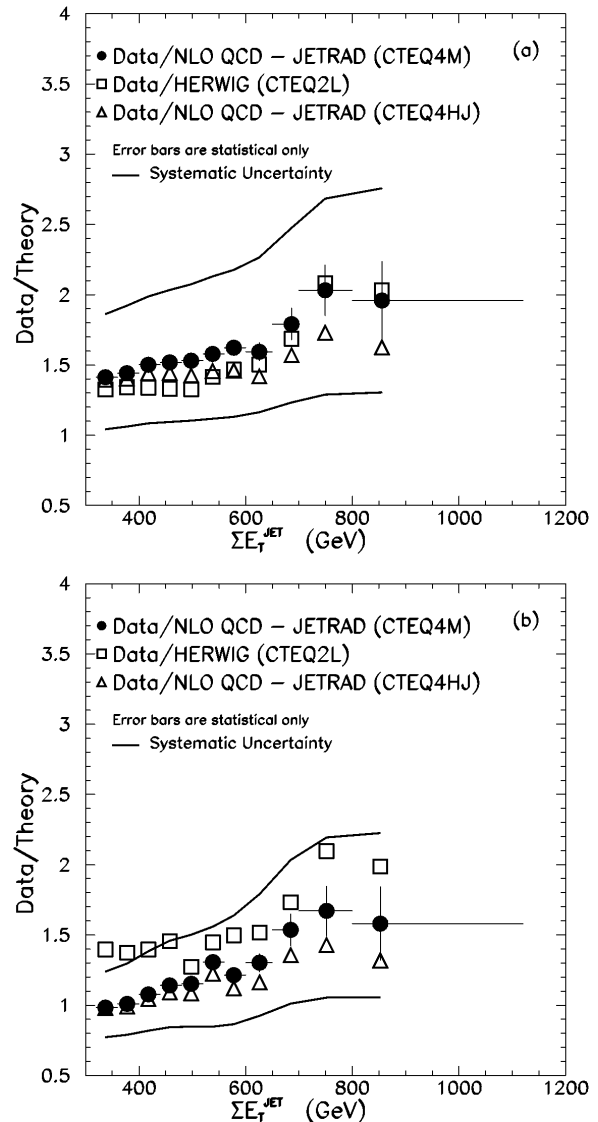


FIG. 2. The unsmeared $\sum E_T^{\text{jet}}$ cross section divided by HERWIG and by NLO QCD (DATA/THEORY). Each set of points is DATA/THEORY using different parton distributions as indicated on the figure. The error bars are shown on only one set of points for the sake of clarity. The systematic uncertainties are shown with respect to the solid points. (a) $E_T^{\text{min}} = 20$ GeV, (b) $E_T^{\text{min}} = 100$ GeV.

with NLO QCD using the MRSA [13] and GRV94 [14] parton distributions yield similar normalizations and shapes.

Recently, the CDF high- E_T^{jet} (>200 GeV) inclusive jet data have been included in the CTEQ4HJ global parton distribution fits [15]. With respect to the predictions using the previous PDFs, an increase of 25–30% in the cross section at high E_T^{jet} is predicted due to an increase in the gluon density in the proton. Figure 2 shows the data divided by the theoretical predictions for the CTEQ4HJ PDF. The ratio at high $\sum E_T^{\text{jet}}$ is reduced by about a factor of 1.25 relative to CTEQ4M for both E_T^{min} values.

In summary, we have measured the differential cross section ($d\sigma/d\sum E_T^{\text{jet}}$) for two different E_T^{min} choices using a sample of events whose kinematic properties have been previously found to be in agreement with predictions from LO QCD [1–5]. For the $E_T^{\text{min}}(100)$ sample, which is dominated by two-jet events, the observed event rate is well reproduced by the NLO QCD calculation. The $E_T^{\text{min}}(20)$ sample is no longer dominated by two-jet topologies, and there is a larger dependence of the predictions on the choice of renormalization and factorization scale. Given this uncertainty, there is reasonable agreement between the data and the predictions (1.14 standard deviations). The HERWIG parton shower Monte Carlo underestimates the event rate for both E_T^{min} values, presumably because the predicted cross section is based on the LO $2 \rightarrow 2$ scattering matrix element. Compared to current NLO QCD predictions these spectra exhibit an excess of events at large $\sum E_T^{\text{jet}}$ which is similar to the excess we have previously reported in the inclusive jet cross section. Use of the new parton distribution functions that include the high- E_T^{jet} jet data decreases the disagreement by about 25%.

We thank the Fermilab Accelerator Division and the technical and support staff of the participating institutions

for their vital contributions. This work was supported by the U.S. Department of Energy and the National Science Foundation; the Instituto Nazionale di Fisica Nucleare of Italy; the Ministry of Science, Culture and Education of Japan; the Natural Sciences and Engineering Research Council of Canada; the National Science Council of the Republic of China and the A. P. Sloan Foundation.

*Visitor.

- [1] CDF Collaboration, F. Abe *et al.*, Phys. Rev. D **45**, 2249 (1992).
- [2] CDF Collaboration, F. Abe *et al.*, Phys. Rev. Lett **75**, 608 (1995).
- [3] CDF Collaboration, F. Abe *et al.*, Phys. Rev. D **54**, 4221 (1996).
- [4] G. Marchesini and B. Webber, Nucl. Phys. **B310**, 461 (1988). Version 5.6 was used for this measurement
- [5] F. A. Berends and H. Kuijf, Nucl. Phys. **B353**, 59 (1991).
- [6] W. T. Giele, E. W. N. Glover, and D. A. Kosower, Nucl. Phys. **B403**, 633 (1993). Version 1.0 was used for this measurement.
- [7] CDF Collaboration, F. Abe *et al.*, Phys. Rev. Lett. **76**, 3070 (1996).
- [8] CDF Collaboration, F. Abe *et al.*, Nucl. Instrum. Methods Phys. Res., Sect. A **271**, 387 (1988).
- [9] CDF Collaboration, F. Abe *et al.*, Phys. Rev. D **45**, 1448 (1992).
- [10] CDF Collaboration, F. Abe *et al.*, Phys. Rev. Lett. **70**, 1376 (1993).
- [11] CDF Collaboration, F. Abe *et al.*, Phys. Rev. Lett. **77**, 438 (1996).
- [12] H. L. Lai *et al.*, Phys. Rev. D **55**, 1280 (1997).
- [13] A. D. Martin, R. G. Roberts, and W. J. Stirling, Phys. Rev. D **50**, 6734 (1994).
- [14] M. Glück, E. Reya, and R. Vogt, Z. Phys. C **67**, 433 (1995).
- [15] H. L. Lai and W. K. Tung, hep-ph/9605269, 1996; J. Huston *et al.*, Phys. Rev. Lett. **77**, 444 (1996).